

# Micromachined metallic thin films for the gas diffusion layer of PEFCs

Kazuyoshi Fushinobu\*, Daishi Takahashi, Ken Okazaki

*Department of Mechanical and Control Engineering, Tokyo Institute of Technology, Meguro-ku, Tokyo 152-8552, Japan*

Received 1 September 2005; received in revised form 23 October 2005; accepted 25 October 2005

Available online 28 November 2005

## Abstract

Feasibility and the design parameter effect are examined for micromachined metallic thin film gas diffusion layer (GDL) for polymer electrolyte fuel cells (PEFCs). Titanium thin film is used at present due to its endurance to the cell operation. Cell operation characteristics under various humidification and cell temperature behavior are examined to show the importance of water management. Impact of design parameters such as through-hole diameter, through-hole patterning and the thin film thickness have been investigated to show the parameter dependence as well as the possible high performance with design optimization. The GDL is expected to be used for rigorous modeling of overpotential factors.  
© 2005 Elsevier B.V. All rights reserved.

*Keywords:* PEMFC; Gas diffusion layer; Thin film; Micromachining

## 1. Introduction

Polymer electrolyte fuel cell (PEFC) has been gaining enormous attentions due to its possible applications in automobile, stationary and mobile power sources. For instance, Japanese Ministry of Economy, Trade and Industry (METI) is taking an initiative of fuel cells and hydrogen-based energy research, development and introduction package where the launch of FCV fleet and stationary power sources with co-generation system are expected. As the development proceeds, more and more attentions are paid to the basic science of fuel cells, such as the degradation issues.

The authors have been conducting fundamental investigations associated with the electrochemical reaction and transport phenomena in a PEFC single cell. Fundamental catalytic reaction on Pt and Pt-3d transition metal alloy catalysts and the mechanism of high reactivity in alloy catalysts have been investigated by means of *ab initio* molecular analysis and X-ray absorption spectroscopy as well as basic electrochemical characterization [1,2]. Also, the molecular and ionic transport characteristics in the polymer electrolyte membrane and the possible high transport property with ordered molecular structure have been studied with classical molecular dynamics calculations [3]. At the cell-

level, the thermal and water content field in the MEA have been visualized by using thermography and infrared optical absorption technique [4,5], and a rigorous numerical calculation that considers the conjugate nature of electrochemical reaction and transport phenomena has been conducted in order to understand the complex behavior of cell operation [6]. Based on these understandings, various cell level studies have been conducted, such as the catalyst degradation mechanism [7].

There have been through these efforts, importance of a priori modeling of the diffusion resistance in the gas diffusion layer (GDL) and the resulting concentration overpotential has gained big attention due to the difficulty of modeling regular GDLs with extremely complex pore structure. There have been many works proposed associated with the overpotential at the GDL [8,9]. Previous models, however, either model the concentration overpotential by using the limiting current density that is defined to be the current density at zero cell voltage to predict the *i*-*V* characteristics [10], or to use a fitting parameter to describe the diffusion resistance through the GDL in CFD-based analysis [11]. These approaches are very useful when a PEFC cell or a stack needs modeling of its operation characteristics once the fitting parameters are determined from experiment. However, the extremely complex structure of regular GDLs, such as carbon paper or carbon cloth, prevents a development of a priori modeling of concentration overpotential through the concentration profile prediction by means of diffusion analysis. Lattice Boltzmann method is recently applied to model the complicated

\* Corresponding author. Tel.: +81 3 5734 2500; fax: +81 3 5734 2893.  
E-mail address: [fushinok@mech.titech.ac.jp](mailto:fushinok@mech.titech.ac.jp) (K. Fushinobu).

### Nomenclature

|                    |  |
|--------------------|--|
| $i$                | current density ( $\text{A m}^{-2}$ )          |
| $i_{\text{limit}}$ | limiting current density ( $\text{A m}^{-2}$ ) |
| $T_{\text{cell}}$  | cell temperature ( $^{\circ}\text{C}$ )        |
| $t$                | thickness of Ti GDLs (m)                       |
| $V$                | voltage (V)                                    |

### Greek letter

|        |  |
|--------|--|
| $\phi$ | diameter of through-holes in Ti GDLs (m) |
|--------|--|

### Subscripts

|   |         |
|---|---------|
| a | anode   |
| c | cathode |

phenomena in GDLs for simplified structure [12], and the applicability is still limited. For instance, by using a PEFC cell with a novel GDL that allows a priori modeling, one can separately calculate the overpotentials in order to more rigorously investigate the cell-level phenomena.

In this study, we propose a novel GDL that has highly ordered porous structure prepared by using the micromachining technique, which helps a priori modeling of concentration overpotential at GDLs. Metallic thin films with on the order of  $10^{-6}$  to  $10^{-5}$  m thickness are micromachined in order to equip with columnar vertical micro through-holes in thickness direction. The simple GDL structure allows mass transfer based modeling of concentration overpotential, which helps to rigorously analyze the other overpotential factors. Also, by replacing the carbon-based GDLs with metallic thin films, the thickness and electrical resistivity are both reduced on the order of magnitudes to suggest the possibility of high performance GDLs.

The objective of this work is to exhibit the feasibility and the design parameter impact of this micromachined metallic thin film as a GDL on a single cell PEFC operation. Operation performance with various design parameter GDLs is examined from  $i$ - $V$  curves (polarization curves.)

## 2. Experimental set-up

### 2.1. GDL sample fabrication

The thin film GDLs are fabricated by using regular micromachining technique. Fig. 1 shows the process flow of fabricating a Ti GDL sample:

- (1) A titanium thin film is diced so that it fits the size of the test cell shown in Fig. 4.
- (2) Aluminum is deposited on the titanium thin film by an RF magnetron sputtering machine (SANYU, SVC-700RF II). The aluminum layer is used as a sacrificial layer for the RIE etching of titanium.
- (3) Photoresist coating by using spin-coater and pre-baked.
- (4) Photolithographic patterning of the photoresist and post-baked.

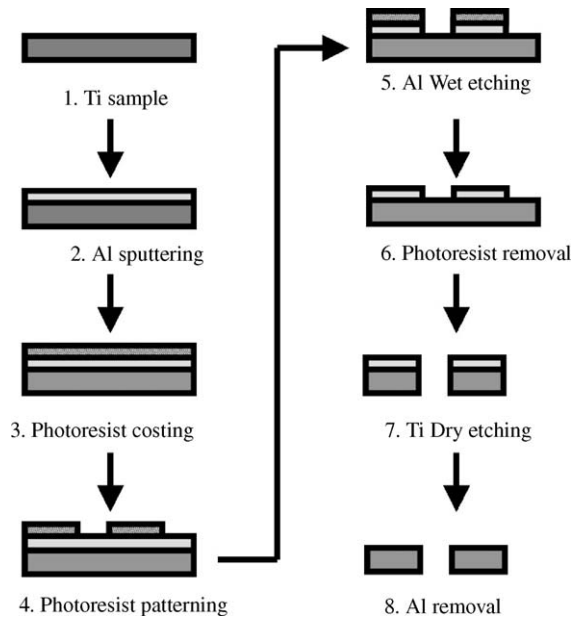


Fig. 1. Micromachining process flow of Ti GDL fabrication.

- (5) The aluminum layer is wet-etched.
- (6) The photoresist is removed.
- (7) The titanium thin film is etched by using RIE (SAMCO, RIE-101L) to create micro through-holes.
- (8) The aluminum layer is removed by using wet etching.

By using the process, Ti thin film GDLs with micro through-holes are fabricated, and Fig. 2 shows a top view of a typical Ti GDL sample image with 25- $\mu\text{m}$  diameter through-holes. Although the GDL samples with various through-hole diameter,  $\phi$ , and the titanium thin film thickness,  $t$ , are prepared and examined in the following experiment, the number of through-holes,  $N$ , are prepared so that the porosity of the GDL in a single gas channel region (width:  $W = 1$  mm, length:  $L = 10$  mm) has same value of porosity that is defined as the volume of through-

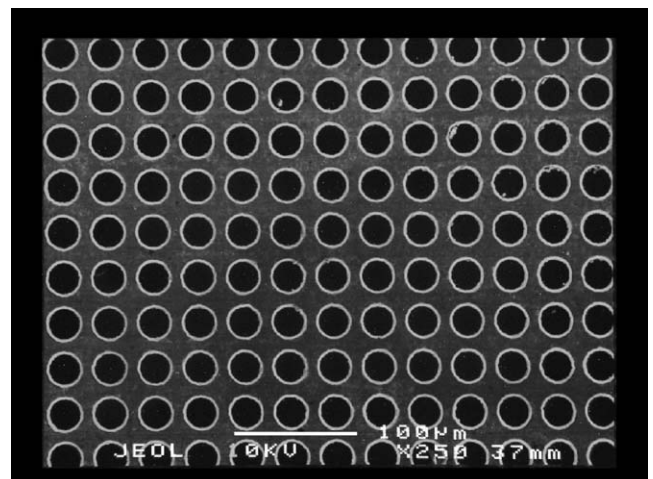


Fig. 2. SEM image of a Ti GDL top view with 25- $\mu\text{m}$  diameter micro through-holes.

Table 1  
Relation between the through-hole diameter and the number of through-holes in a gas channel region

| Through-hole diameter ( $\mu\text{m}$ ) | Number of through-holes in span-wise direction in a gas channel region | Number of through-holes in flow-wise direction in a gas channel region | Number of through-holes in a gas channel region |
|---|--|--|---|
| 10                                      | 65   | 665  | 43225   |
| 25                                      | 26   | 266  | 6916  |
| 50                                      | 13   | 133  | 1729  |

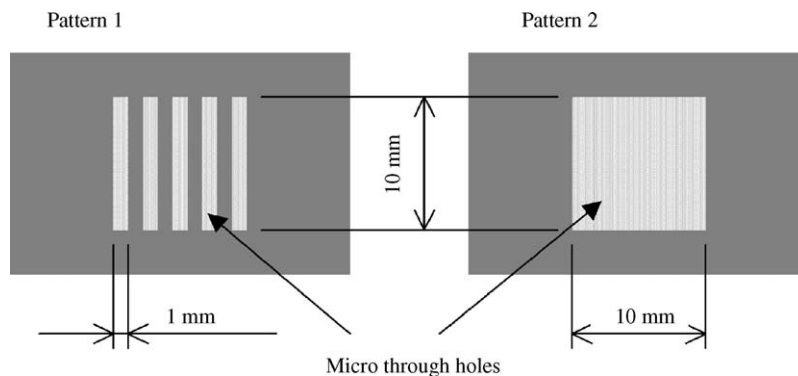


Fig. 3. Micro through-hole fabrication patterns. Only in the gas channel region has through holes in Pattern 1, while Pattern 2 has in both gas channel and separator rib regions.

holes ( $=Nt\pi\phi^2/4$ ) divided by the volume of the GDL ( $=tWL$ ). A gas diffusion layer is attached to a separator that has (1) gas channels where the supply gas and generated  $\text{H}_2\text{O}$  flow (termed as “gas channel region” of a GDL in this manuscript) and (2) so called ribs where the electrical current is collected from/to the GDL to give it to/from the external load (“rib region”). Table 1 shows the number of through-holes in a gas channel region for various through-hole diameters, and the porosity is 0.339 in all cases.

In order to examine the effect of transport characteristics at the rib region, we have prepared two different patterns of through-hole fabrication as shown in Fig. 3. In Pattern 1 in Fig. 3, only the gas channel region (1 mm  $\times$  10 mm, five channels) has through holes, while the Pattern 2 has through-holes both in the gas channel and the rib regions.

## 2.2. Test cell

Fig. 4(a) shows the test section of the experimental set-up. The cell consists of GDLs, separators that have gas channels on the GDL sides and a catalyst coated membrane (CCM) in

between the GDLs. As well as Ti GDLs previously described, commercially available carbon paper GDL (Japan Goretex, CABEL) with a thickness of about 300  $\mu\text{m}$  is used as a reference case. Fig. 4(b) shows a schematic of a separator that describes the gas channel geometry. Separators have gas channels as shown in the figure, and the square area surrounded by the dotted line corresponds to the catalyst coated area (10 mm  $\times$  10 mm) of the CCM. Commercially available CCM (Japan Goretex, PRIMEA) is used in the experiment.

Hydrogen and oxygen are introduced to the cell as shown in Fig. 4(a) and supplied to the catalyst layers on the membrane through the GDLs. Flow rate and the humidity of the gasses are controlled by using mass flow controllers and humidifiers. The cell temperature is defined to be the temperature without cell operation and is controlled by changing the temperature of a chamber in which the cell is placed. A parameter set of a typical operation condition is as follows unless otherwise specified:  $\text{H}_2$  flow rate: 20 ml  $\text{min}^{-1}$ ,  $\text{O}_2$  flow rate: 20 ml  $\text{min}^{-1}$ , cell temperature: 20  $^\circ\text{C}$  and no humidification. Cell voltage is measured at various current density values to examine the characteristics of the Ti GDLs.

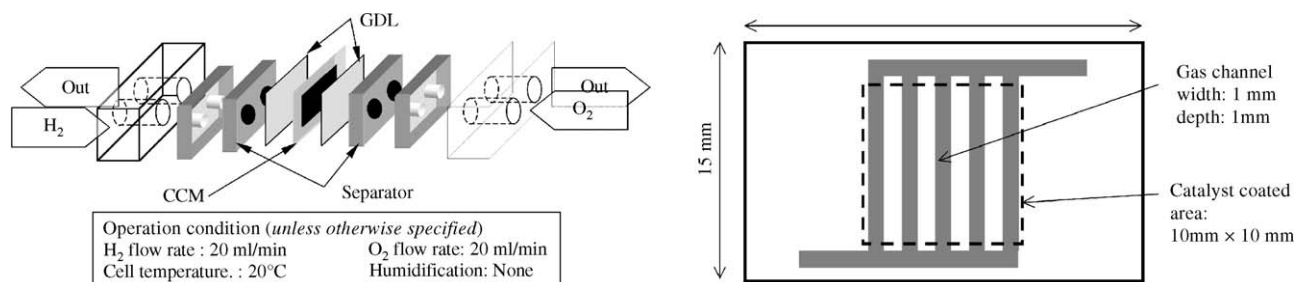


Fig. 4. A schematic of experimental set-up: (a) a schematic of test cell, (b) separator schematic.

### 3. Results and discussions

#### 3.1. Effect of operation parameters

Fig. 5(a)–(c) shows the  $i$ – $V$  characteristics of the cell with Ti GDLs. In these experiments, titanium thin film GDLs with through-hole Pattern 1 is employed. Thickness of Ti thin film is  $5\ \mu\text{m}$ , both anode- and cathode-side GDLs have through-hole diameter of  $50\ \mu\text{m}$  and the flow rate of  $\text{H}_2$  and  $\text{O}_2$  are  $50\ \text{ml}\ \text{min}^{-1}$ . Effect of humidification is examined at both 100% RH (relative humidity) and without humidification cases under various cell temperatures.

Fig. 5(a) shows the  $i$ – $V$  curve at cell temperature of  $40\ ^\circ\text{C}$ , and the results show that the cell performance degrades at 100% RH. This is due to the condensation and the resulting water flooding in GDLs due to the relatively low cell temperature. With higher RH humidification, the condensation and flooding more likely to occur than the case without humidification. This trend can also be understood from the fact that the  $i$ – $V$  curve drops at relatively high current density where the more  $\text{H}_2\text{O}$  generation is expected and therefore the concentration overpotential is more significant.

Fig. 5(b) shows the  $i$ – $V$  curve at relatively high cell temperature,  $T_{\text{cell}} = 60\ ^\circ\text{C}$ . In this case, the cell performance improves with increasing humidification, contrary to  $T_{\text{cell}} = 40\ ^\circ\text{C}$  case. By rising the cell temperature, more evaporation of  $\text{H}_2\text{O}$  from the membrane to the gas channel through the GDL is expected, and the GDL flooding due to the humidification is less likely to take place. Other behavior to be noted is the increase of the limiting current density,  $i_{\text{limit}}$ , where the cell voltage becomes zero. This is due to the decrease of membrane ohmic resistance

and concentration resistance. Change of the gradient of the  $i$ – $V$  curve indicates the decrease of the membrane resistance.

The same humidity dependence is more significantly observed from Fig. 5(c) at much higher cell temperature,  $T_{\text{cell}} = 80\ ^\circ\text{C}$ . The discrepancy between two humidification conditions increases in Fig. 5(c). Comparison of the  $i$ – $V$  curve gradient with  $T_{\text{cell}} = 60\ ^\circ\text{C}$  case indicates the increase of membrane resistance at without humidification. It is expected from the results that the evaporation of  $\text{H}_2\text{O}$  from the membrane becomes more significant due to the high temperature, and that the cell performance drastically decreases without humidification. Comparison of the  $i$ – $V$  curve gradient of Fig. 5(b) and (c) at 100% RH indicates the decrease of membrane resistance. The limiting current density, however, is identical at both cases to suggests that the concentration overpotential determines  $i_{\text{limit}}$ .

#### 3.2. Effect of design parameters

In order to examine the effect of GDL design parameters, through-hole diameter of the cathode-side GDL,  $\phi_c$ , through-hole patterning and the GDL thickness,  $t$ , is varied and the resulting  $i$ – $V$  curve is presented in Figs. 6–8.

Fig. 6 shows the effect of the cathode-side through-hole diameter,  $\phi_c$ , of the Ti GDL. The anode-side through-hole diameter,  $\phi_a$ , is  $50\ \mu\text{m}$  in all cases, and the GDL thickness is  $5\ \mu\text{m}$  at both sides. The figure clearly exhibits the increasing cell performance with decreasing through-hole diameter. Change of the  $i$ – $V$  curve gradient indicates the decrease of the ohmic overpotential. This can be understood by considering the following effects: Although the surface area at which the catalyst coated area is

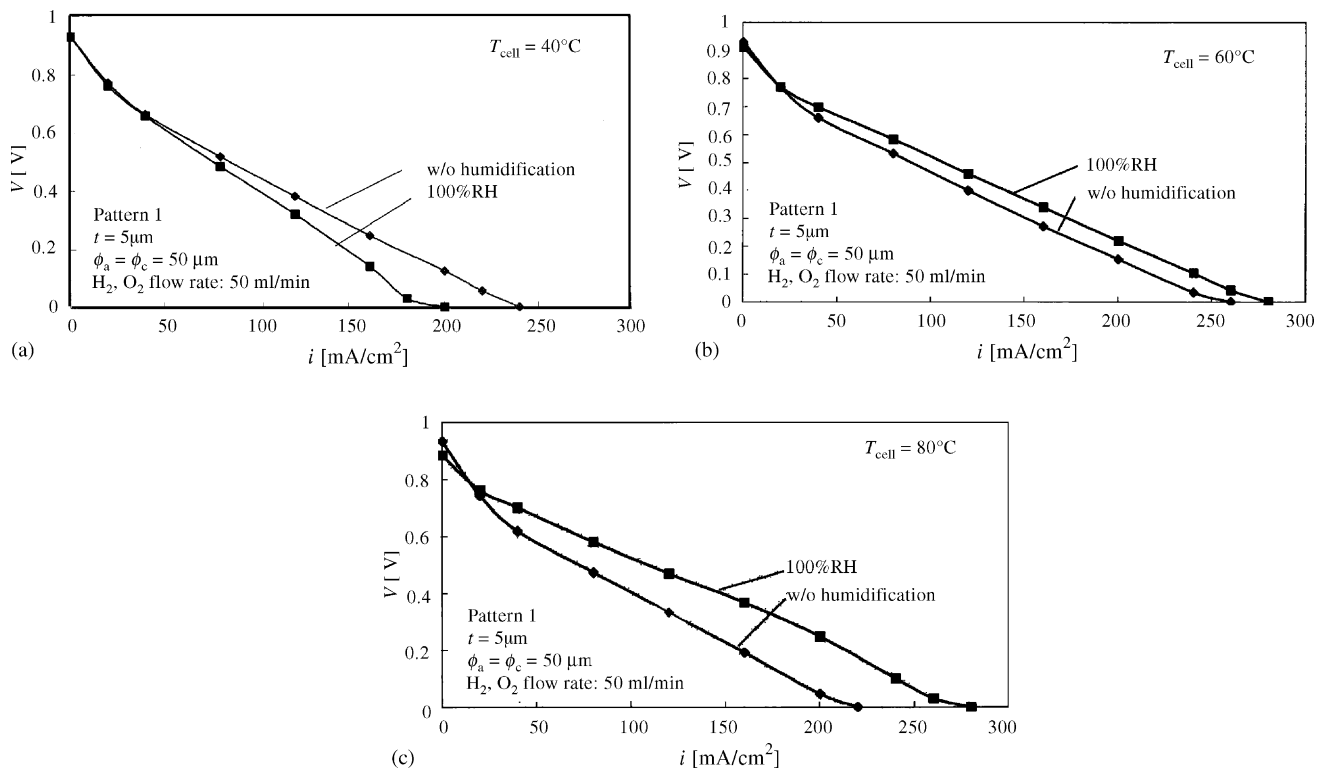


Fig. 5.  $i$ – $V$  curve of Ti thin film GDL. Effect of cell temperature and humidification. (a)  $T_{\text{cell}} = 40\ ^\circ\text{C}$ , (b)  $T_{\text{cell}} = 60\ ^\circ\text{C}$ , (c)  $T_{\text{cell}} = 80\ ^\circ\text{C}$ .

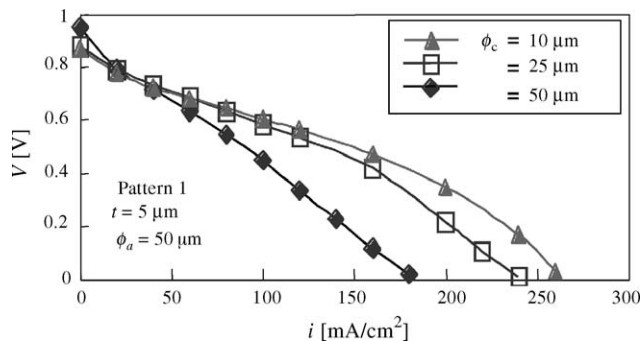


Fig. 6.  $i$ - $V$  curve of Ti thin film GDL. Effect of cathode-side through-hole diameter.

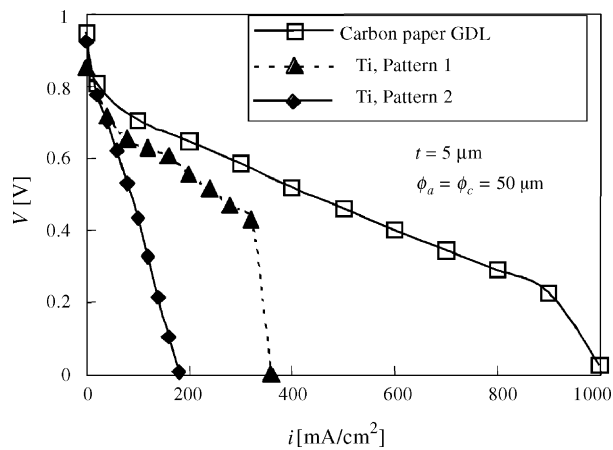


Fig. 7.  $i$ - $V$  curve of Ti thin film GDL. Effect of through-hole region pattern.

directly exposed to the gas channel through the through-holes,  $N\pi\phi_c^2$ , is the same regardless of the value of  $\phi_c$ , and therefore the expected surface area at which the catalytic reaction takes place is also the same value of  $N\pi\phi_c^2$ , certain amount of supplied gas may spread in between the GDL and the catalyst layer from the hole edge to increase the surface area where the electrochemical reaction takes place,  $A_{\text{eff}}$ . Assuming a constant gas spreading length from the hole edge,  $d_{\text{sp}}$ , and considering the constant value of  $N\pi\phi_c^2$  as described in the sample fabrication section, decrease of through-hole diameter leads to the increase

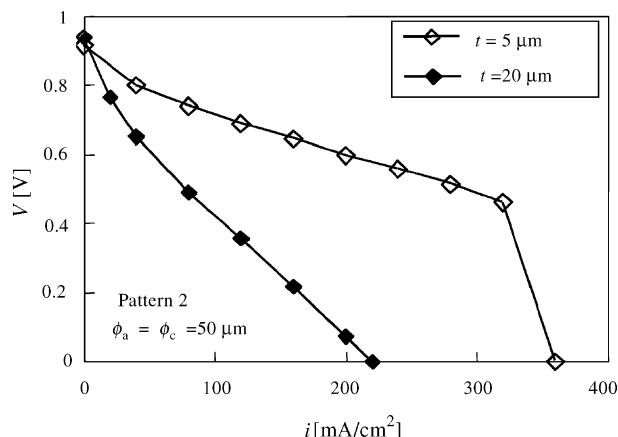


Fig. 8.  $i$ - $V$  curve of Ti thin film GDL. Effect of GDL thickness.

of  $A_{\text{eff}}$  as

$$A_{\text{eff}} = N\pi(\phi_c + d_{\text{dp}})^2 = N\pi\phi_c^2 \left(1 + \frac{d_{\text{dp}}}{\phi_c}\right)^2. \quad (1)$$

Also, the electrical resistivity of the catalyst coated area can be larger than that of the Ti film. Therefore, the increase of through-hole diameter means the increase of the in-place electrical resistance in the catalyst coated area through the increase of electrical conduction length.

The results discussed in the preceding paragraph are the data of Pattern 1 GDL where the through-holes only exist in the gas channel region, as shown in Fig. 3. The rib region is also expected to work as an electrochemically active area in PEFCs since the regular GDLs, such as carbon papers or carbon cloths, allow the mass transport from/to the gas channel not only to the gas channel region but also to the rib region due to their complex porous structure. Fig. 7 compares the cell performance of Ti GDLs with different patterns (Patterns 1 and 2) and that of commercially available carbon paper GDL. Through-hole diameter is 50  $\mu\text{m}$ , and the Ti GDL thickness is 5  $\mu\text{m}$ . Titanium GDL of Pattern 2 shows significant increase of the cell performance compared with Pattern 1. The results indicate that the rib area of the catalyst also contributes to the electrochemical reaction. Also, further performance improvement of thin film GDL can be expected since the design parameters are not yet optimized.

The performance improvement, however, cannot be observed when the GDL thickness of Pattern 2 is increased to 20  $\mu\text{m}$  as shown in Fig. 8. The result for  $t = 20 \mu\text{m}$  is close to the result of Pattern 1 in Fig. 7. Although the GDL thickness is 4 times larger, the potential drop across the GDL thickness of 20  $\mu\text{m}$  at current density of 200  $\text{mA cm}^{-2}$  is only on the order of  $10^{-8}$  V. Considering the identical trend with the data of Pattern 1 with  $t = 5 \mu\text{m}$  in Fig. 7, the poor performance may be attributed to inability of gas supply to the rib region.

#### 4. Conclusions

Characteristics of highly ordered porous GDLs have been investigated experimentally. Feasibility of applying the structure to be used as GDLs in PEFC is examined, and the effects of various operation parameters have been investigated. Humidification is found to improve the  $i$ - $V$  characteristics at higher operation temperature and to degrade at lower operation temperature. When the porosity is kept constant, smaller through-hole diameter and thinner titanium thickness is found to improve the cell performance. The through-hole patterning is found to be designed carefully. Based on these experimental results, future study is needed to develop a theoretical modeling of concentration overpotential at the GDL and to evaluate the overpotential factors separately.

#### Acknowledgments

This work has been partly supported by the Grant-in-Aid for Encouragement of Young Scientists (A) (No. 15686010) from the Japan Society for the Promotion of Science (JSPS).

Part of sample fabrication has been conducted at the Mechano-Micro Process Lab of Tokyo Institute of Technology. The authors greatly acknowledge their support.

## References

- [1] K. Okazaki, R. Kokubu, K. Fushinobu, Y. Uchimoto, Reaction mechanisms on the Pt-based cathode catalyst for PEFCs – QMD and XAFS analyses for atomic and electronic structures, in: Proceedings of the 15th World Hydrogen Energy Conference 2004, Paper No. 29K-01, 2004.
- [2] K. Okazaki, N. Koiwa, K. Fushinobu, Y. Uchimoto, Surface electronic/atomic structure and reactivity enhancement of alloy catalyst for PEFC, in: Proceedings of the 6th KSME-JSME Thermal and Fluids Engineering Conference 2005, 2005, p. cI.05.
- [3] R. Jinnouchi, K. Okazaki, Molecular Dynamics Study of Transport Phenomena in Perfluorosulfonate Ionomer Membrane for PEFC, *J. Electrochem. Soc.* 150 (2003) E66–E73.
- [4] R. Shimoi, M. Masuda, K. Fushinobu, Y. Kozawa, K. Okazaki, Visualization of the membrane temperature field of a polymer electrolyte fuel cell, *ASME J. Energy Resour. Technol.* 126 (4) (2004) 258–261.
- [5] K. Fushinobu, K. Shimizu, N. Miki, K. Okazaki, Optical measurement technique of water contents in polymer membrane for PEFCs, *ASME J. Fuel Cell Sci. Technol.*, in press.
- [6] M. Masuda, Y. Kozawa, H. Sato, K. Fushinobu, K. Okazaki, Coupling phenomena of electrochemical reaction and heat transport in polymer electrolyte fuel cell, *J. Jpn. Soc. Mech. Eng. (Kikai Gakkai Ronbunshuu, in Japanese)* B68 (665) (2002) 209–217.
- [7] N. Miki, K. Fushinobu, K. Okazaki, Impact of operation parameters on MEAs in a PEFC cell, in: Proceedings of the JSME Thermal Engineering Conference 2004 (Japanese), 2004, pp. 415–416.
- [8] T. Hottinen, M. Mikkola, T. Mennola, P. Lund, Titanium sinter as gas diffusion backing in PEMFC, *J. Power Sources* 118 (2003) 183–188.
- [9] G.G. Park, Y.J. Sohn, T.H. Yang, Y.G. Yoon, W.Y. Lee, C.S. Kim, Effect of PTFE contents in the gas diffusion media on the performance of PEMFC, *J. Power Sources* 131 (2004) 182–187.
- [10] M.L. Perry, J. Newman, E.J. Cairns, Mass transport in gas-diffusion electrodes: a diagnostic tool for fuel-cell cathodes, *J. Electrochem. Soc.* 145 (1998) 5–15.
- [11] H. Masuda, K. Ito, T. Masuoka, Y. Kakimoto, Investigation of water blocking phenomena in PEMFC by numerical analysis, in: Proceedings of the JSME Thermal Engineering Conference 2004 (Japanese), 2004, pp. 31–32.
- [12] S. Hirai, M. Sakaguchi, K. Nishida, S. Tsushima, Water transport analysis in a porous electrode in PEFC by LBM simulation, in: Proceedings of the 42nd National Heat Transfer Symposium of Japan (Japanese), 2005, pp. 93–94.